

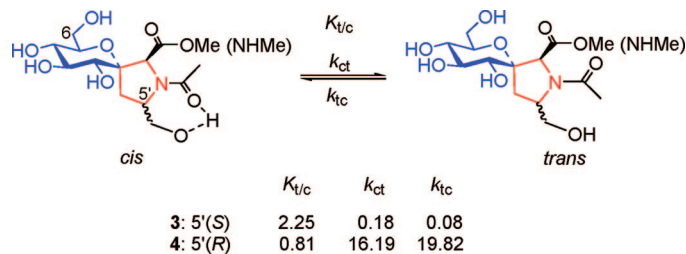
Intramolecular Hydrogen Bond-Controlled Prolyl Amide Isomerization in Glucosyl 3'(S)-Hydroxy-5'-hydroxymethylproline Hybrids: Influence of a C-5'-Hydroxymethyl Substituent on the Thermodynamics and Kinetics of Prolyl Amide *Cis/Trans* Isomerization

Kaidong Zhang,[†] Robel B. Teklebrhan,[†] G. Schreckenbach,[†] Stacey Wetmore,[‡] and Frank Schweizer^{*,†}

Department of Chemistry, University of Manitoba, Winnipeg, Manitoba R3T 2N2, Canada, and Department of Chemistry & Biochemistry, University of Lethbridge, Lethbridge, Alberta T1K 3M4, Canada

schweize@cc.umanitoba.ca

Received February 16, 2009



Peptide mimics containing spirocyclic glucosyl-(3'-hydroxy-5'-hydroxymethyl)proline hybrids (Glc3'(S)-5'(CH₂OH)HypHs) with a polar hydroxymethyl substituent at the C-5' position, such as C-terminal ester Ac-Glc3'(S)-5'(CH₂OH)Hyp-OMe and C-terminal amide Ac-Glc3'(S)-5'(CH₂OH)Hyp-N'-CH₃, were synthesized. C-Terminal esters exhibit increased *cis* population (23–53%) relative to Ac-3(S)Hyp-OMe (17%) or Ac-Pro-OMe (14%) in D₂O. The prolyl amide *cis* population is further increased to 38–74% in the C-terminal amide form in D₂O. Our study shows that the stereochemistry of the hydroxymethyl substituent at the C-5' position of proline permits tuning of the prolyl amide *cis/trans* isomer ratio. Inversion–magnetization transfer NMR experiments indicate that the stereochemistry of the hydroxymethyl substituent has a dramatic effect on the kinetics of prolyl amide *cis/trans* isomerization. A 200-fold difference in the *trans*-to-*cis* (k_{tc}) isomerization and a 90-fold rate difference in the *cis*-to-*trans* (k_{ct}) isomerization is observed between epimeric C-5' **3** and **4**. When compared to reference peptide mimics Ac-Pro-OMe and Ac-3(S)Hyp-OMe, our study demonstrates that a (13–16)-fold decrease in k_{tc} and k_{ct} is observed for the C-5'(S), while a (5–24)-fold acceleration is observed for the C-5'(R) epimer. DFT calculations indicate that the pyrrolidine ring prefers a C^β *exo* pucker in both Ac-Glc3'(S)-5'(CH₂OH)Hyp-OMe diastereoisomers. Computational calculations and chemical shift temperature coefficient ($\Delta\delta/\Delta T$) experiments indicate that the hydroxymethyl group at C-5' in Ac-Glc3'(S)-5'(CH₂OH)Hyp-OMe forms a stabilizing intramolecular hydrogen bond to the carbonyl of the N-acetyl group in both epimeric *cis* isomers. However, a competing intramolecular hydrogen bond between the hydroxymethyl groups in the pyrrolidine ring and pyran ring stabilizes the *trans* isomer in the C-5'(S) diastereoisomer. The dramatic differences in the kinetic properties of the diastereoisomeric peptide mimics are rationalized by the presence or absence of an intramolecular hydrogen bond between the hydroxymethyl substituent located at C-5' and the developing lone pair on the nitrogen atom of the N-acetyl group in the transition state.

Introduction

Proline (Pro) is the only cyclic amino acid of the 20 DNA-encoded amino acids which is characterized by limited rotation

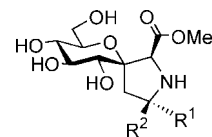
of the ϕ dihedral angle (fixed at $\sim -75^\circ$) as its side chain is fused to the peptide backbone. As a result, there is a reduction in the energy difference between the prolyl amide *cis*- and *trans*-isomers making them nearly isoenergetic; this leads to a higher *cis* N-terminal amide content relative to the other amino acids. The kinetics of the prolyl *cis/trans* isomerization reaction is the

[†] University of Manitoba.

[‡] University of Lethbridge.

rate-determining step in the folding pathways of many peptides and proteins.¹ Moreover, proline induces β -turns and extended helical structures (polyproline helix) in peptides that are crucial in protein/protein and protein/peptide interactions.² In nature, proline undergoes post-translational modifications such as hydroxylation to 4(*R*)-hydroxyproline (4-Hyp) and 3(*S*)-hydroxyproline (3-Hyp).^{3–6} Hydroxylation of proline is critical to the thermal stability and modulation of the local stability of the triple helix in collagens⁷ and contributes to the stability of the poly-Hyp helix in plant-derived Hyp-rich glycopeptides.⁸

Over the years, a plethora of proline analogues such as C ^{β} -, C ^{γ} - and C ^{δ} -substituted prolines,^{9–12} azaprolines,¹³ pseudoproline,¹⁴ silaprolin,¹⁵ proline–amino acid chimera,¹⁶ fused bicyclic proline,^{17–19} and fused glucose–proline analogues²⁰ have been developed to study the structural and biological properties of proline surrogates in peptides.²¹ In particular, pseudoproline bearing two substituents adjacent to the endocyclic nitrogen of proline and C ^{δ} -substituted prolines containing bulky substituents have been shown to increase the prolyl amide *cis* conformer ratio in peptides and peptide mimics.^{9,21c,22} Incorporation of pseudoproline into peptides has been shown



1: R¹ = CH₂OH; R² = H

2: R¹ = H; R² = CH₂OH

FIGURE 1. Structure of spirocyclic glucose-3(*S*)-hydroxy-5'-hydroxymethylproline hybrids (Glc3'(*S*)-5'-(CH₂OH)HypHs).

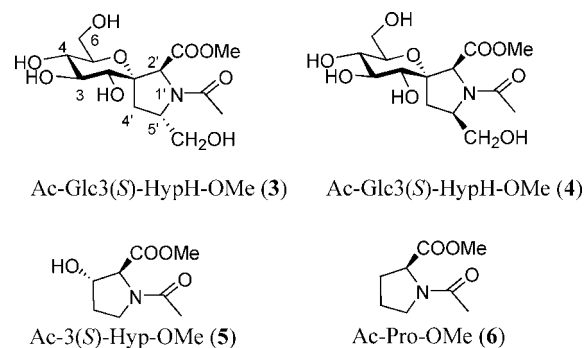


FIGURE 2. Peptide mimics 3–6. C-Terminal esters 3 and 4 are the glucose-3'(*S*)-hydroxy-5'(*S*)-hydroxymethylproline analogue and glucose-3'(*S*)-hydroxy-5'(*R*)-hydroxymethylproline analogue while esters 5 and 6 serve as reference compounds.

to induce a “kink” conformation in the peptide backbone, originating in the preference for *cis* amide bond formation. This prevents peptide aggregation, self-association, and β -structure formation, thus improving the solvation and coupling kinetics of the growing peptide chain considerably.²³

Recently, we have reported on the synthesis of spirocyclic glucose-3(*S*)-hydroxy-5'-hydroxymethylproline hybrids (Glc3'(*S*)-5'-(CH₂OH)HypHs) 1 and 2 (Figure 1).²⁴ Compounds 1 and 2 exhibit several intriguing features. The spirocyclic nature of the *gluco*-derived scaffold constrains the pyrrolidine ring of proline and introduces artificial post-translational modifications (hydroxylation + glycosylation). Chemical manipulations and derivatizations of the glucose-derived polyol scaffold provide an opportunity to tailor the chemical, physical, and pharmacodynamic properties of Glc3'(*S*)-5'-(CH₂OH)HypHs-containing peptides.²⁵ Moreover, compounds 1 and 2 contain a hydroxymethyl substituent adjacent to the imino function of proline which may permit control of prolyl amide *cis/trans* isomerization via hydrogen bonding, electrostatic, or steric interactions. It is noteworthy that the influence of C-5'-substituted proline analogues capable of forming polar interactions on the thermodynamics and kinetics of prolyl amide *cis/trans* isomerization has not yet been investigated.

Results

Herein, we describe the thermodynamics and kinetics of prolyl *N*-terminal amide isomerization of peptide mimics 3 and 4 (Figure 2). Compounds 5 and 6 serve as reference compounds and were selected to study how 3(*S*)-hydroxylation of proline

(23) Wöhr, T.; Wahl, F.; Nefzi, A.; Rohwedder, B.; Sato, T.; Sun, X.; Mutter, M. *J. Am. Chem. Soc.* **1996**, *118*, 9218.

(24) Zhang, K.; Schweizer, F. *Synlett* **2005**, 3111.

(25) Gruner, S. W.; Locardi, E.; Lohof, E.; Kessler, H. *Chem. Rev.* **2002**, *102*, 491.

(26) Jenkins, C. L.; Bretscher, L. E.; Guzei, I. A.; Raines, R. T. *J. Am. Chem. Soc.* **2003**, *125*, 6422.

(1) (a) Brandits, J. F.; Halvorson, H. R.; Brennan, M. *Biochemistry* **1975**, *14*, 4953. (b) Schmid, F. X.; Baldwin, R. L. *Proc. Nat. Acad. Sci. U.S.A.* **1978**, *75*, 4764. (c) Hurlle, M. R.; Marks, C. B.; Kosen, P. A.; Anderson, S.; Kuntz, I. D. *Biochemistry* **1990**, *29*, 4410. (d) Jackson, S. E.; Fersht, A. R. *Biochemistry* **1991**, *30*, 10436.

(2) (a) Stryer, L. *Biochemistry*, 4th ed.; W. H. Freeman and Co.: New York, 1999. (b) Kakinoki, S.; Hirano, Y.; Oka, M. *Polym. Bull. (Berlin)* **2005**, *53*, 109.

(3) Reddy, K. V. R.; Yedery, R. D.; Aranha, C. *Int. J. Antimicrob. Agents* **2004**, *24*, 536.

(4) Buku, A.; Faulstich, H.; Wieland, T.; Dabrowski, J. *Proc. Natl. Acad. Sci. U.S.A.* **1980**, *77*, 2370.

(5) Nakajima, T.; Volcani, B. E. *Science* **1969**, *164*, 1400.

(6) Taylor, S. W.; Waite, J. H.; Ross, M. M.; Shabanowitz, J.; Hunt, D. F. *J. Am. Chem. Soc.* **1994**, *116*, 10803.

(7) (a) Berg, R. A.; Prockop, D. J. *Biochem. Biophys. Res. Commun.* **1973**, *52*, 115. (b) Vitagliano, L.; Berisio, R.; Mazzarella, L.; Zagari, A. *Biopolymers* **2001**, *58*, 459, and references cited therein. (c) Holmgren, S. K.; Taylor, K. M.; Bretscher, L. E.; Raines, R. T. *Nature (London)* **1998**, *392*, 666. (d) Bretscher, L. E.; Jenkins, C. L.; Taylor, K. M.; deRider, M. L.; Raines, R. T. *J. Am. Chem. Soc.* **2001**, *123*, 777. (e) Jenkins, C. L.; Raines, R. T. *Nat. Prod. Rep.* **2002**, *19*, 49.

(8) Pearce, G.; Ryan, C. A. *J. Biol. Chem.* **2003**, *278*, 30044, and references cited therein.

(9) Beausoleil, E.; Lubell, W. D. *J. Am. Chem. Soc.* **1996**, *118*, 12902, and references therein.

(10) Delaney, N. G.; Madison, V. J. *J. Am. Chem. Soc.* **1982**, *104*, 6635.

(11) Samanen, J.; Zuber, G.; Bean, J.; Eggleston, D.; Romoff, T.; Kopple, K.; Saunders, M.; Regoli, D. *Int. J. Pept. Protein. Res.* **1990**, *35*, 501.

(12) Quancard, J.; Labonne, A.; Jacquot, Y.; Chassaing, G.; Lavielle, S.; Karoyan, P. *J. Org. Chem.* **2004**, *69*, 7940.

(13) Che, Y.; Marshall, G. R. *J. Org. Chem.* **2004**, *69*, 9030, and references cited therein.

(14) Tam, J. P.; Miao, Z. *J. Am. Chem. Soc.* **1999**, *121*, 9013, and references cited therein.

(15) Cavellier, F.; Vivet, B.; Martinez, J.; Aubry, A.; Didierjean, C.; Vicherat, A.; Marraud, M. *J. Am. Chem. Soc.* **2002**, *124*, 2917, and references cited therein.

(16) Sharma, R.; Lubell, W. D. *J. Org. Chem.* **1996**, *61*, 202, and references cited therein.

(17) Jeannotte, G.; Lubell, W. D. *J. Org. Chem.* **2004**, *69*, 4656.

(18) (a) Wagaw, S.; Rennels, R. A.; Buchwald, S. L. *J. Am. Chem. Soc.* **1997**, *119*, 8451. (b) Kuwano, R.; Sato, K.; Kurokawa, T.; Karube, D.; Ito, Y. *J. Am. Chem. Soc.* **2000**, *122*, 7614. (c) Viswanathan, R.; Prabhakaran, E. N.; Plotkin, M. A.; Johnston, J. N. *J. Am. Chem. Soc.* **2003**, *125*, 163.

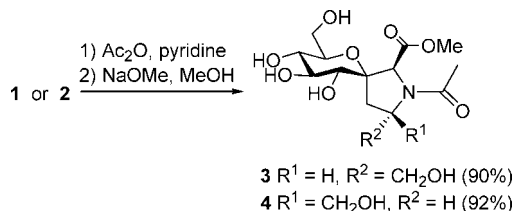
(19) Koep, S.; Gais, H.-J.; Raabe, R. *J. Am. Chem. Soc.* **2003**, *125*, 13243, and references cited therein.

(20) Owens, N.; Braun, C.; Schweizer, F. *J. Org. Chem.* **2007**, *72*, 4635.

(21) For selected examples of bicyclic proline analogues incorporated into bioactive peptides, see: (a) Cluzeau, J.; Lubell, W. D. *Biopolymers, Peptide Science* **2005**, *80*, 98. (b) Blankley, C. J.; Kaltenbronn, J. S.; DeJohn, D. E.; Wener, A.; Bennett, L. R.; Bobowski, G.; Krolls, U.; Johnson, D. R.; Pearlman, W. M.; Hoefle, M. L. *J. Med. Chem.* **1987**, *30*, 992. (c) Dumy, P.; Keller, M.; Ryan, D. E.; Rohwedder, B.; Wöhr, T.; Mutter, M. *J. Am. Chem. Soc.* **1997**, *119*, 918. (d) Li, W.; Moeller, K. D. *J. Am. Chem. Soc.* **1996**, *118*, 10106.

(22) Keller, M.; Sager, C.; Dumy, P.; Schutkowski, M.; Fisher, G. S.; Mutter, M. *J. Am. Chem. Soc.* **1998**, *120*, 2714. And references therein.

SCHEME 1. Synthesis of Peptide Mimics 3 and 4



influences the kinetics and thermodynamics of prolyl amide *cis/trans* isomerization. We initially selected *C*-terminal methyl esters to avoid complications arising from competing intramolecular hydrogen bonding of *C*-terminal amides.²⁷ Furthermore, the amide bond order of 3–6 can be assessed by FT-IR without interference with *C*-terminal amide. Subsequently, we extended our study to *C*-terminal methylamides.

Synthesis of Peptide Mimics 3–6. Peptide mimics 3 and 4 were synthesized by acetylation of proline analogues 1 and 2 in pyridine and acetic anhydride followed by *O*-deacetylation using a solution of sodium methoxide in methanol (Scheme 1). Peptide mimic 5 was synthesized according to a modified procedure,²⁶ while peptide mimic 6 was purchased.

Assignments of *N*-Terminal Geometry for Both Major and Minor Isomers of 3 and 4 and Determination of K_{tc} . Identification of prolyl amide *trans* and *cis* isomers were based on multiple one-dimensional GOESY²⁸ experiments in CD₃OD in which the optimized resolution was obtained (Figure 3). For instance, subtraction of the H-2' signal in prolyl amide *cis* isomer 3a to a one-dimensional GOESY experiment showed interproton effect to the *N*-terminal methyl group (5.2% NOE relative to the H-2' signal). By comparison, no interproton effect was observed between H-5' and the *N*-terminal methyl group. The same diagnostic tools were used to assign the prolyl amide isomers in compounds 3b, 4a, and 4b, and the observed interproton effects are summarized in Figure 3.

We also observed that the ¹³C NMR chemical shifts of the *C*-2' atoms of the *trans* rotamers in compounds 3 and 4 are high-field shifted (0.8–1.6 ppm) relative to the *cis* isomers irrespective of the solvent used (Table 1). For instance, in methanol, we observed *C*-2' for *cis* isomer 3a at 72.80 ppm, while the *trans* isomer 3b appeared at 71.74 ppm in the ¹³C NMR. This result is consistent with previous findings by Lubell⁹ and may serve as an empirical rule to assign the prolyl amide *cis* and *trans* isomers in cases where GOESY experiments cannot be performed.

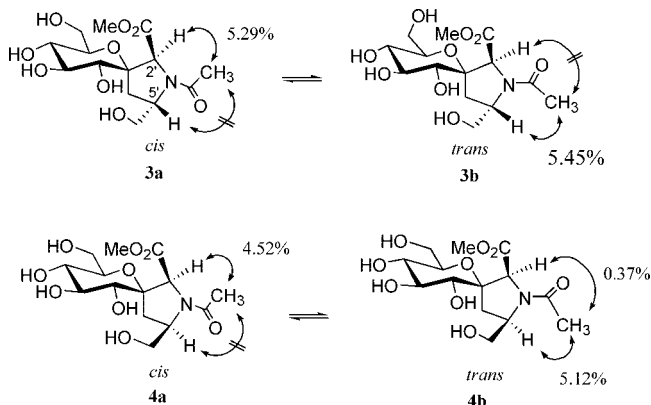


FIGURE 3. Assignment of *cis* and *trans* isomers in compounds 3 and 4 in CD₃OD through 1D NOE.

TABLE 1. Chemical Shift of *C*-2' in *Cis* and *Trans* Isomers of 3 and 4

compd		3 ^a	4 ^a	3 ^b	4 ^b
<i>C</i> -2' (ppm)	<i>cis</i>	73.63	73.55	72.80	72.67
	<i>trans</i>	72.66	72.30	71.74	71.08

^a Measured in D₂O. ^b Measured in CD₃OD.

TABLE 2. *Trans/Cis* Ratio^a K_{tc} (± 0.04) and (*cis*% $\pm 3\%$) Isomers of 3–6 in Water

compd	3	4	5	6
K_{tc} (<i>cis</i> %)	3.35 (23%)	0.88 (53%)	4.88 (17%)	6.14 (14%)

^a Determined by 500 MHz NMR at 25 °C.

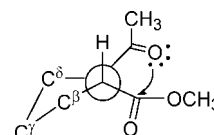


FIGURE 4. $n \rightarrow \pi^*$ interaction (looking down *C*^α–*N* bond).

For each compound 3–6, the ratio of *trans/cis* isomers was calculated by integrating and averaging as many well-resolved proton signals as possible in the ¹H NMR spectra (Table 2).²⁹ We found that the hydroxymethyl substituent at *C*-5' enables tuning of the prolyl amide *cis/trans* ratio. For instance, compound 4 shows a slight preference for the *cis* rotamer (53%) while its *C*-5' epimer exists predominantly as the *trans* rotamer (77%). In comparison, reference compounds 5 and 6 exhibit nearly identical *cis/trans* ratios confirming that the presence of an electron-withdrawing hydroxyl group in 5 has no measurable effect on the prolyl amide *cis/trans* rotamer population.²⁶

In order to compare our results with other reported proline analogues, we converted peptide esters 3 and 4 into *N*-methylamides 7 and 8 by nucleophilic displacement (Supporting Information). Peptide mimics 7 and 8 show a significantly increased *cis* rotamer population when compared to esters 3 and 4. Similar observations have been made by others, and these results have been explained by enhanced $n \rightarrow \pi^*$ interactions³⁰ of the oxygen lone pair of the (*i* – 1) *trans* amide residue to the antibonding orbital of the C=O bond belonging to the Pro (*i*) residue (Figure 4).²⁹ The fact that an amide carbon is less electron deficient^{30b} than an ester carbon has been used to explain higher *trans* ratios in prolyl amide of *C*-terminal esters when compared to the prolyl amide of *C*-terminal amides.²⁹

The *cis* population of peptide mimics 7 and 8 is presented in Table 3 together with previously published data for proline analogue 9,⁹ 5-methylproline analogues 10 and 11,³¹ and 5-*tert*-butylproline analogues 12 and 13 (Figure 5).⁹ These results show that 8 induces a high *cis* rotamer population (74 \pm 3%) while 7 exhibits a reduced *cis* rotamer population (38 \pm 3%). Interestingly, the stereochemistry at *C*-5' of 7 and 8 seems to have a reverse effect on the equilibrium constant of isomeriza-

(27) (a) Cox, C.; Lectka, T. *J. Am. Chem. Soc.* **1998**, *120*, 10660. (b) Mizushima, S.; Shimanouchi, T.; Tsuboi, M.; Sugita, T.; Kurosaki, K.; Mataga, N.; Souda, R. *J. Am. Chem. Soc.* **1952**, *74*, 4639. (c) Liang, G. B.; Rito, C. J.; Gellman, S. H. *Biopolymers* **1992**, *32*, 507.

(28) A 40 ms Gaussian pulse with a 560 ms mixing time was used.

(29) Taylor, C. M.; Hardre, R.; Edwards, P. J. B.; Park, J. H. *Org. Lett.* **2003**, *23*, 4413, and references cited therein.

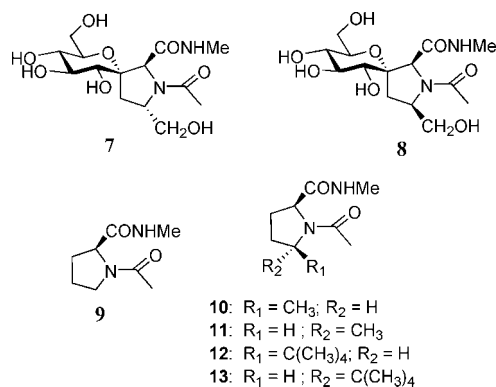
(30) (a) DeRider, M. L.; Wilkens, S. J.; Waddell, M. J.; Bretscher, L. E.; Weinhold, F.; Raines, R. T.; Markley, J. L. *J. Am. Chem. Soc.* **2002**, *124*, 2497. (b) Hinderaker, M. P.; Raines, R. T. *Protein Sci.* **2003**, *12*, 1188. (c) Hodges, J. A.; Raines, R. T. *Org. Lett.* **2006**, *8*, 4695.

(31) Delaney, N. G.; Madison, V. *Int. J. Peptide Protein Res.* **1982**, *19*, 543.

TABLE 3. Cis Population of Prolyl *N*-Acetyl-*N'*-methylamides in D₂O

compd	7	8	9 ^a	10 ^b	11 ^b	12 ^a	13 ^a
<i>cis</i> (±3%)	38	74	27	25	30	49	66

^a Taken from ref 9. ^b Taken from ref 31.

**FIGURE 5.** Various *N*-acetyl *N'*-methylamides. Compounds 9–13 have been previously synthesized.^{9,31}**TABLE 4.** Rate Constants of Prolyl Amide Isomerization for 3–6

amide	k_{ct} ^a (s ⁻¹)	k_{tc} ^b (s ⁻¹)
3	0.18 ± 0.01	0.08 ± 0.004
4	16.19 ± 1.19	19.82 ± 1.45
5	2.63 ± 0.28	1.02 ± 0.09
6	2.95 ± 0.12	0.82 ± 0.04

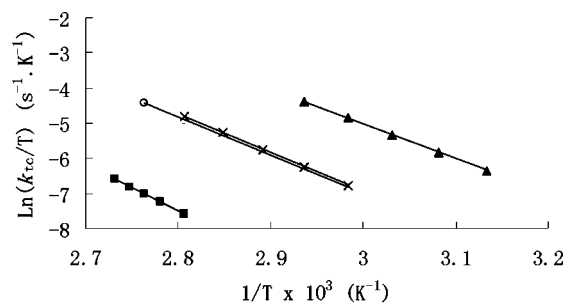
^a Carried out in D₂O at 83 °C. ^b Calculated from k_{ct} and K_{tc} .

tion by comparison with *tert*-butyl proline analogues **12** and **13** (Table 3).

Kinetics of *Cis*–*Trans* Prolyl Amide Bond Isomerization in Peptide Mimics 3–6. The kinetics of *cis/trans* isomerization for compounds **3**–**6** were determined by ¹H NMR spectroscopy inversion–magnetization transfer experiments³² in D₂O (Table 4). Because the rates for *cis/trans* isomerization are extremely slow in protic solvents, we performed these experiments at elevated temperatures.³³ At 83 °C, the *trans*-to-*cis* rate constants of isomerizations (k_{tc}) follow the order **4** < **5** ≈ **6** < **3**. A 200-fold rate difference is observed for diastereomeric amides **3** and **4**. In comparison, hydroxyprolyl amide **5** and prolyl amide **6** exhibit nearly identical rate constants, indicating that the 3(*S*)-hydroxy group has little effect on the kinetics of isomerization.

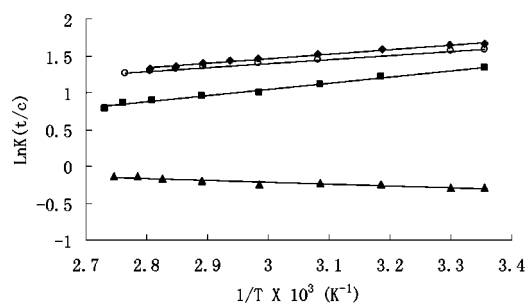
The effects of temperature on k_{ct} and k_{tc} were analyzed by Eyring plots (Figure 6).³⁴ The values for ΔH^\ddagger and ΔS^\ddagger (Table 5) were calculated from linear least-squares fits of the data in these plots.³⁴ The activation parameters demonstrate that the free energy barriers to isomerization of compounds **3**–**6** are enthalpic in origin. Interestingly, amide **3** exhibits a significantly increased activation enthalpy (3.9–6.8 kcal/mol) when compared to compounds **4**–**6**. However, the activation enthalpy is partially compensated by a higher activation entropy.

Thermodynamics. The effects of temperature on the values $K_{tc} = (k_{ct}/k_{tc})$ for each compound were measured directly by NMR spectroscopy over the temperature range 25–93 °C. The resulting data were analyzed by Van't Hoff plots (Figure 7).

(32) (a) Perrin, C. L.; Dwyer, T. J. *Chem. Rev.* **1990**, *90*, 935. (b) Reimer, U.; Scherer, G.; Drewello, M.; Kruber, S.; Schutkowski, M.; Fischer, G. *J. Mol. Biol.* **1998**, *279*, 449.(33) Stein, R. L. *Adv. Protein Chem.* **1993**, *44*, 1.(34) Eyring, H. *J. Chem. Phys.* **1935**, *3*, 107.**FIGURE 6.** Eyring plots: *trans*-to-*cis* (up); *cis*-to-*trans* (down); compounds **3** (■), **4** (▲), **5** (○), and **6** (×).**TABLE 5.** Activation Enthalpies (ΔH^\ddagger) and Entropies (ΔS^\ddagger) as Derived from Eyring Plots in D₂O for 3–6 and Free Energies of Activation at 298 K (ΔG^\ddagger)

	<i>cis</i> to <i>trans</i> ^a			<i>trans</i> to <i>cis</i> ^a		
	ΔH^\ddagger ^b	ΔS^\ddagger ^c	ΔG^\ddagger ^c	ΔH^\ddagger ^b	ΔS^\ddagger ^c	ΔG^\ddagger ^c
3	26.1	11.1	22.8	26.4	10.2	23.4
4	19.8	2.2	19.1	19.6	1.9	19.0
5	21.6	3.6	20.5	21.5	1.6	21.1
6	21.9	4.8	20.5	22.5	3.9	21.4

^a Error limits obtained from the residuals of the linear least-squares fitting of the data to equation, $\ln(k/T) = (-\Delta H^\ddagger/R)(1/T) + \Delta S^\ddagger/R + \ln(k_B/h)$, were 1–3% for ΔH^\ddagger in compounds **3**–**6**, 3–7% for ΔS^\ddagger in **3** and **6**, 16–26% for ΔS^\ddagger in **4**, and 19–48% for ΔS^\ddagger in **5**; ^b Units: kcal/mol. ^c Units: cal/mol.K. ^c Units: kcal/mol.

**FIGURE 7.** Van't Hoff plots for compounds **3** (■), **4** (▲), **5** (○), and **6** (◆) in D₂O.**TABLE 6.** Thermodynamic Parameters for Isomerization of 3–6

amide	ΔH° ^a (kcal/mol)	ΔS° ^a (cal/mol·K)	ΔG° ^b (298 K)
3	−1.67 ± 0.06	−2.93 ± 0.20	−0.80 ± 0.13
4	0.50 ± 0.06	1.05 ± 0.16	0.19 ± 0.11
5	−1.09 ± 0.03	−0.48 ± 0.08	−0.95 ± 0.05
6	−1.21 ± 0.04	−0.71 ± 0.12	−1.01 ± 0.08

^a Error limits obtained by linear least-squares fitting the data of the Van't Hoff plots to equation $\ln K_{tc} = (-\Delta H^\circ/R)(1/T) + \Delta S^\circ/R$. ^b Carried out in D₂O; ± SE determined by integration of two or more sets of *trans/cis* isomers.

Amides **3**, **5**, and **6** have a positive slope indicating that the major *trans* isomer becomes increasingly favored as the temperature decreases. However, compound **4** displays a negative slope and shows a reduction in the magnitude of K_{tc} . In this case, the major *cis* isomer becomes increasingly favored as the temperature decreases. Values for ΔH° and ΔS° were calculated from linear least-squares fits of these plots (Table 6).

FT-IR Analysis of Amide I Band (C=O Stretching) for 3–6 in D₂O. We also measured the frequency of the amide I vibrational mode, which results primarily from the C=O

TABLE 7. Temperature Coefficient ($\Delta\delta/\Delta T$, ppb/K) for Compounds **3** and **4** in DMSO- d_6

		HO-2	HO-3	HO-4	HO-6	HO-6'
3	<i>cis</i>	-6.87	-6.49	-5.85	-5.29	-3.94
	<i>trans</i>	-6.98	-6.94	-5.67	-5.14	-4.13
4	<i>cis</i>	-7.58	-6.94	-5.85	-5.48	-3.75
	<i>trans</i>	-6.94	-6.57	-5.55	-4.92	-4.50

stretching vibration.³⁵ The traditional picture of the amide resonance predicts that an increase in C=O bond order is accompanied by a decrease in C-N bond order. Such a decrease in C-N bond order would facilitate *cis/trans* isomerization of the amide bond. In D₂O, the amide I vibrational modes of **6**, **3**, **5**, and **4** are at 1608, 1609, 1612, and 1613 cm⁻¹, respectively, and follow the order **6** ~ **3** < **5** ~ **4**. It has been shown that changes in the free energy of activation (ΔG^\ddagger) for prolyl peptide bond isomerization are proportional to changes in the frequency (ν) of the amide I vibrational mode.³⁶ Our results demonstrate that 3-Hyp-based amide **5** is blue-shifted ($\Delta\nu = 4$ cm⁻¹) when compared to prolyl amide **6**. However, these subtle differences are not detectable by our kinetic assay. A similar trend is observed for spirocyclic amides **3** and **4**. Obviously, the blue shift ($\Delta\nu = 4$ cm⁻¹) observed for **4** is too small to account for the significant changes in ΔG^\ddagger between **3** and **4**, and this suggests that other factors unrelated to inductive effect and C=O bond order are the cause for this dramatic rate difference.³⁶

Temperature Coefficient ($\Delta\delta/\Delta T$) Measurement of OH Resonances for **3 and **4** in DMSO- d_6 .** We next considered the effect of hydrogen bonding on prolyl amide *cis/trans* isomerization. The temperature coefficients ($\Delta\delta/\Delta T$) provide information about intramolecular hydrogen bonding.³⁷ Previous studies have shown that ($\Delta\delta/\Delta T$) > -3.0 ppb/deg are a diagnostic tool for the detection of intramolecular H-bonding.³⁷ The 1D spectra of compounds **3** and **4** recorded between 20 to 45 °C in 5-deg steps in DMSO- d_6 were analyzed, and the temperature coefficients were determined (Table 7). Our data show that the temperature coefficients for HO-6' exhibit the highest value of all hydroxyl groups. The temperature coefficients follow the general order OH-2 < OH-3 < OH-4 < OH-6 < OH-6'. In particular, the low ($\Delta\delta/\Delta T$) value for the *cis* isomers in **3** (-3.94 ppb/K) and **4** (-3.75 ppb/K), respectively, suggests the presence of intramolecular H-bonding involving OH-6'. In the *trans* isomers of **3** and **4**, the $\Delta\delta/\Delta T$ of HO-6' were reduced to -4.13 and -4.50 ppb/K, respectively. The relatively small value of HO-6' in both *trans* isomers of **3** and **4** indicates that it also could be involved in hydrogen bonding for both compounds.

Conformational Analysis of the Pyrrolidine Ring in **3 and **4** Using Density Functional Theory (DFT).** In order to gain insight into the conformational properties of peptide mimics **3** and **4** in solution and to study how intramolecular hydrogen-bonding influences the kinetics and thermodynamics of prolyl amide isomerization in compounds **3** and **4**, we performed DFT calculations. On the basis of previous experience and literature reviews,^{38,39} we selected the B3LYP level of theory,⁴⁰⁻⁴² which

TABLE 8. The Calculated Distribution (%) of *Cis* and *Trans* Conformers for **3** and **4** in D₂O^a

	compd	calcd	exptl
3	<i>cis</i>	29.15	23 ± 3
	<i>trans</i>	70.85	77 ± 3
4	<i>cis</i>	57.75	53 ± 3
	<i>trans</i>	42.25	47 ± 3

^a Calculations at the B3LYP/ B3LYP/6-31+G(d, p)/PCM level of theory.

has been shown good enough to provide accurate predictions of molecular structures, and the 6-31+G(d, p) basis set,⁴³ which is a relatively large basis set augmented by diffuse and polarization functions to account for correlation effects. Additionally, solvent effects were taken into account using Tomasi's polarized continuum model (PCM).⁴⁴ In this model, the solvent is represented as a polarizable medium characterized by its dielectric constant (i.e., water has a dielectric constant of 78.4 at 25 °C and 1 atm), and the solute molecules are placed in a cavity within the solvent.

A multistep procedure was used to determine the structures of **3** and **4** to ensure that our calculations covered the entire conformational space. First, the conformational space was searched using the MMFF (molecular mechanics) force field and a Monte Carlo search procedure, which was augmented by systematically varying the initial starting structure. After the resulting conformers were superimposed to remove duplicates, 443 and 457 unique structures, respectively, for compounds **3** and **4** were found at the MMFF level. These conformers were used as input for gas-phase DFT optimizations, which were subsequently followed by solvation optimizations. The final Gibbs free energies were calculated and compared to determine the (Boltzmann) distribution of *cis* and *trans* isomers, which are summarized in Table 8. Full details on the computational protocol can be found in the Supporting Information.

The calculated distribution of prolyl amide *cis/trans* isomers in compounds **3** and **4** is in good agreement with the experimental data determined by ¹H NMR integration (Table 8). For compound **4**, the *cis* isomer population was calculated to be 57.7%, while the experimentally determined value is 53 ± 3%. A slightly weaker agreement is observed for **3**. In this case, the calculated *cis* ratio is 29%, while the experimental value is 23 ± 3%.

In terms of structure, the computational data show that the pyranose ring in **3** and **4** exists in a ⁴C₁ chair conformation consistent with the diaxial coupling constants $J_{2,3}$, $J_{3,4}$, $J_{4,5} \geq 8.8$ Hz observed in the ¹H NMR. The range of peptide backbone (ω' , ϕ , ψ , and ω) and endocyclic torsion angles (χ^0 , χ^1 , χ^2 , χ^3 , and χ^4) for peptide mimics **3** and **4** are displayed in Table 9. Full details for all conformers can be found in the Supporting Information. With the exception of the ψ torsion angle that exists in two families at $\psi \sim 153^\circ$ and $\psi \sim -28^\circ$, all other torsion angles show preference for only one narrowly defined range. Values close to 0° for the ω' torsion angles define the *cis* prolyl

(35) Jackson, M.; Mantsch, H. H. *Crit. Rev. Biochem. Molec. Biol.* **1995**, 30, 95.

(36) Eberhardt, E. S.; Panatik, N., Jr.; Raines, R. T. *J. Am. Chem. Soc.* **1996**, 118, 12261.

(37) (a) Leeflang, B. R.; Vliegthart, J. F. G.; Kroon-Batenburg, L. M. J.; Eijck, B. P.; Kroon, J. *Carbohydr. Res.* **1992**, 230, 41. (b) St-Jacques, M.; Sundarajan, P. R.; Taylor, K. J.; Marchessault, R. H. *J. Am. Chem. Soc.* **1976**, 98, 4386.

(38) Koch, W.; Holthausen, M. C. *A Chemist's Guide to Density Functional Theory*, 2nd ed.; Wiley: Weinheim, 2000.

(39) Cramer, C. J. *Essentials of Computational Chemistry: Theories and Models*, 2nd ed.; Wiley: New York, 2004.

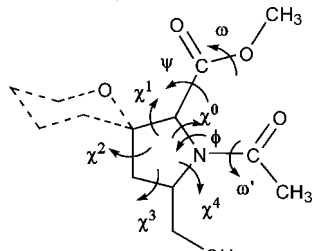
(40) Becke, A. D. *J. Chem. Phys.* **1993**, 98, 5684.

(41) Lee, C.; Yang, W.; Parr, R. G. *Phys. Rev. B: Condens. Matter* **1988**, 37, 785.

(42) Stephens, P. J.; Devlin, F. J.; Chabalowski, C. F.; Frisch, M. J. *J. Phys. Chem.* **1994**, 98, 11623.

(43) Hehre, W. J. *A Guide to Molecular Mechanics and Quantum Chemical Calculations*; Wavefunction, Inc.: Irvine, CA, 2003; p 393.

(44) Tomasi, J.; Mennucci, B.; Cammi, R. *Chem. Rev.* **2005**, 105, 2999.

TABLE 9. Range of Backbone and Endocyclic Torsion Angles⁴⁵ (deg) for the Most Stable Conformers of **3** and **4** Accounting for 99.5% of the Total Conformer Population Determined by DFT Calculations (Substituents on the Pyran Ring Are Omitted for Clarity)


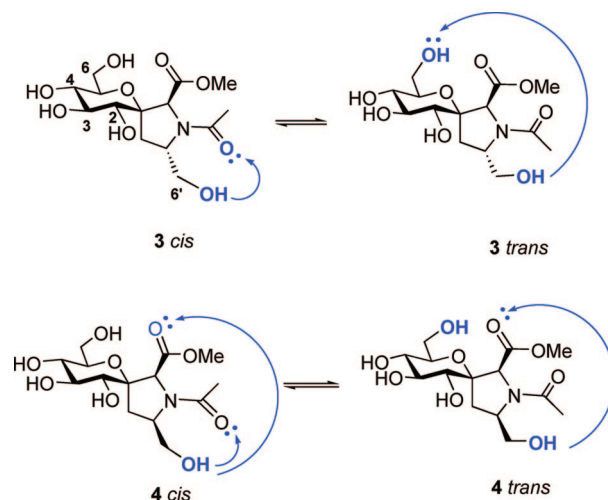
		ω'	ϕ	Ψ	ω	χ^0	χ^1	χ^2	χ^3	χ^4
3	<i>cis</i>	-11, -1	-71, -62	153, 154 -28, -27	177 ± 1 -177 ± 1	-15, -22	30, 34	-35, -33	21, 25	-5, 0
	<i>trans</i>	165, 178	-67, -53	132, 154 -30, -27	178 ± 1 -179 ± 1	-16, -6	25, 30	-36, -34	24, 30	-14, -7
4	<i>cis</i>	3, 12	-91, -77	152, 154 -28, -27	177 ± 1 -177 ± 1	-21, -15	31, 33	-37, -32	20, 27	-8, 0
	<i>trans</i>	-172, -169	-86, -79	152, 154 -28, -26	178 ± 1 -179 ± 1	-21, -19	30, 33	-33, -30	18, 21	-1, 2

amide isomer, while values close to $\pm 180^\circ$ describe the *trans* isomer. The observed small χ^4 torsion angle ($-14^\circ \leq \chi^4 \leq 0^\circ$) for the conformers of compounds **3** and **4** indicate a preferred C^β -exo pucker in which the basal plane is defined by C^γ , C^δ , N, and C^α (Figure 8). Similar puckerings of the pyrrolidine ring have been observed in the crystal structure of 3-Hyp-containing peptide mimics and have also been proposed in 3-Hyp-containing collagenous peptide sequences.²⁶ The relative close value for χ^4 and χ^0 in the *trans* rotamer of **3** indicates a twisted conformation between a C^β -exo and a C^γ -endo pucker. The C^β -exo conformation places the endocyclic oxygen substituent in an axial position as observed for *trans*-3(*S*)-hydroxyproline-containing dipeptides.⁴⁷ In this conformation, the pyrrolidine ring will be stabilized by gauche interaction and a stabilizing $\sigma(C^\gamma-H) \rightarrow \sigma^*(C^\beta-O)$ interaction. This conformation is further supported by characteristic long-range “W” coupling constants ($J \sim 1.0$ Hz) between H-2' and H-4'_{eq} in both isomers of **3** and **4**.

The most stable conformers accounting for 99.5% of the total conformer population in compounds **3** and **4** were analyzed for the presence and absence of characteristic hydrogen bonds. We used a ≤ 2.5 Å bond length cutoff between the hydrogen atom in the donor and the acceptor atom to ensure that only strong hydrogen bonds were selected.⁴⁸ We found two types of hydrogen bonds in the dominant rotamer populations of **3** and **4** (Figure 9). For compound **3**, the first type of hydrogen bond exists between OH-6' and OH-6 ($6'-OH \cdots OH-6$) with an average bond distance of around 1.9 Å. This hydrogen bond is only observed in the *trans* rotamers of **3**. The second type of hydrogen bond exists between OH-6' and the *N*-terminal carbonyl ($6'-OH \cdots O=C-N$). This hydrogen bond has an average bond length of 1.8 Å and is only found in the *cis* rotamers. In addition, a third hydrogen bond with a bond distance of 1.9 Å (not shown in Figure 9) is found between

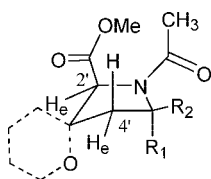
OH-2 and the *C*-terminal carbonyl ($2-OH \cdots O=C'-C-2'$) in one out of the 43 most stable *trans* conformers.

For compound **4**, the first type of hydrogen bond exists between 6'-OH and the *N*-terminal carbonyl ($6'-OH \cdots O=C'-N$). This H-bond has an average distance of 1.8 Å and is found only in the *cis* isomer. A second type of H-bond with a bond length of 1.9 Å exists between 6'-OH and the *C*-terminal carbonyl ($C^\delta-CH_2-OH \cdots O=C'-C-2'$) that is found in both *cis* and *trans* conformers (Figure 9).

**FIGURE 9.** Intramolecular hydrogen bonds in the most stable conformers of the *cis*- and *trans*-isomers of compounds **3** and **4** as determined by DFT (B3LYP/6-31+G(d,p)) calculations in water.

Discussion

The pyrrolidine ring in proline exhibits two predominant pucker modes: *C*-4 (C^γ) *exo* and *endo* envelope conformers. In the case of unsubstituted proline, the *endo* puckering mode is favored over the *exo* mode.⁴⁹ However, the puckering propensity can be controlled by proper choice of ring substituents.⁴⁹ For example, previous studies have shown that introduction of electronegative substituents like 4(*R*)-hydroxy or 4(*R*)-fluoro substituents results in the stabilization of the C^γ -*exo* conformation and the *trans*-prolyl amide isomer.⁵⁰ Our results confirm that naturally occurring 3(*S*)-hydroxyproline does not lead to a measurable increase in the *trans*-prolyl amide isomer popula-



3: R₁ = CH₂OH; R₂ = H
4: R₁ = H; R₂ = CH₂OH;

FIGURE 8. C^β -*exo* conformations of compounds **3** and **4**. The substituents on the glucose ring are omitted for clarity.

tion²⁶ when compared to unsubstituted proline. For the first time, we studied the effect of 3(*S*) hydroxylation on the kinetics of prolyl amide *cis/trans* isomerization. The nearly identical rate constants observed for peptide mimics **5** and **6** at elevated temperature demonstrate that 3(*S*)-hydroxylation has little effect on the kinetics of prolyl amide *cis/trans* isomerization. A similar effect was observed for 4(*R*)-OH proline.⁵⁰ Raines et al. have studied the crystal structure of Ac-3(*S*)-Hyp-OMe **5** and concluded it to be intermediate between a ¹E envelope and ¹E₂ twisted conformation.²⁶ In the envelope conformation the flap atom is C^β (C-3'). In the twisted conformation, atoms N, C^β, and C^δ (C-5') form the basal plane. Atom C^β resides 0.456 ± 0.004 Å above that plane, and C^δ resides 0.153 ± 0.005 Å below that plane.²⁶ Taken together, these results suggest that the hydroxyl group at the β- or γ-position in proline affects the puckering of the pyrrolidine ring in the model peptides without influencing the kinetics and thermodynamics of prolyl amide *cis/trans* isomerization.

These findings are in contrast to our results obtained with Glc3'(S)-5'(CH₂OH)HypHs-containing peptide mimics **3** and **4**. Compounds **3** and **4** demonstrate that kinetics and thermodynamics of *cis/trans* isomerization are greatly affected by the presence of polar groups either by hybridization with D-glucose or incorporation of a hydroxymethyl substituent into the C-5' (δ-)-position of proline. The stereochemistry of the hydroxymethyl substituent at the 5'-position influences both the rate of *cis/trans* isomerization and the stability of the *cis/trans* isomers. Compared to proline and 3(*S*)Hyp-containing peptide mimics **5** and **6**, both Glc3'(S)-5'(CH₂OH)HypHs-modified peptide mimics **3** and **4** display a higher *cis* isomer population. The *cis* isomer population is greatly enhanced in mimic **4**. Substitution of the C-terminal methyl ester in compounds **3** and **4** by a methylamide group increases the *cis* isomer ratio further as expected by enhanced n→π* donation. Indeed, methylamides **7** and **8** exhibit 38% and 74% *cis* isomer, respectively. Comparison of the temperature coefficients for all hydroxyl groups indicates that the increased *cis* prolyl amide isomer ratio in peptide mimics **3**, **4**, **7**, and **8** is hydrogen bond-mediated and involves the hydroxymethyl group located at the C-5' position of proline.

Additional evidence for the involvement of intramolecular hydrogen bonds in the stabilization of the prolyl amide *cis* isomer is provided by detailed DFT conformational searches. Analysis of the most stable prolyl amide *cis* conformers in **3** and **4** indicate the presence of a strong hydrogen bond between 6'-OH and the carbonyl group of NAc (6'-OH---O=C-N). The higher *cis* isomer ratio in **4** is due to the formation of a second hydrogen bond involving 6'-OH and the carbonyl of the carboxymethyl group. Alternatively, the *trans* prolyl amide bond in **3** may be stabilized by the formation of a hydrogen bond between 6'-OH and 6-OH. In addition, the calculations support

the notion that the H-bond between 6'-OH---O=C-N is stronger in compound **4** when compared to **3**. For instance, for compound **4**, 10 out of the 20 most stable conformers possess this type of H-bond, while the same H-bond was not present in the most stable 20 conformers of compound **3**.

Conformational analysis of the pyrrolidine ring in the highly populated conformers in peptide mimics **3** and **4** indicates that the pucker resembles a C^β-exo conformation in both compounds, which is very similar to the conformation previously observed in the crystal structure of **5**. This conformation places the endocyclic oxygen substituent in an axial position as observed for *trans*-3(*S*)-hydroxyproline-containing dipeptides.⁴⁷ In this conformation, the pyrrolidine ring will be stabilized by a gauche interaction between endocyclic nitrogen and endocyclic oxygen and a stabilizing σ(C^γ-H)→σ*(C^β-O) interaction. A similar C^β-exo conformation was also observed in the more lipophilic silaproline (Sip) analogue.¹⁵ However, in this case, no increase of the *cis* isomer population was noted. It is noteworthy that the calculated C^β-exo conformation is closely related to the C^γ-endo pucker that is found in most proline-containing peptides, the polyproline helix, and the collagen triple helix.

Quite unexpected are the results for the kinetics of prolyl amide *cis/trans* isomerization in compounds **3** and **4**. Peptide mimic **3** exhibits an unusually high activation barrier when compared to epimer **4**. For instance, an approximately 200-fold difference in *k*_{tc} and a 90-fold rate difference in *k*_{ct} are observed between compounds **3** and **4**. In contrast, nearly identical rate constants are observed for parent compounds **5** and **6**. Interestingly, while *cis/trans* isomerization is kinetically inhibited in compound **3**, compound **4** accelerates isomerization relative to parent compounds **5** and **6**. For instance, compound **4** exhibits approximately a 6-fold rate acceleration for *k*_{ct} and a 20-fold acceleration for *k*_{tc} when compared to the parent compounds. Comparison of the activation enthalpies and activation entropies of compounds **3**–**6** indicates that enthalpic changes are responsible for these rate differences. Enthalpic changes could be the result of ground- and transition-state stabilization or destabilization.⁵¹

Previous studies by Lubell have shown that introduction of methyl substituents at the β-position in proline and 4-hydroxyproline induced ψ dihedral angles around 150°. This places the C-terminal carbonyl oxygen in a position which disfavors amide pyramidalization by Coulomb interactions in the transition state.⁵² DFT calculations on both compounds **3** and **4** indicate a Ψ dihedral angle around 153° and ~-28° in their most stable conformers which demonstrates that a similar destabilization may exist in peptide mimics **3** and **4**. However, compounds **3** and **4** exhibit dramatic rate differences. We suggest that the presence or absence of intramolecular H-bonds involving 6'-OH, the endocyclic nitrogen and the carboxymethyl group are responsible for the observed rate differences. Computational models on the most stable (ground-state) conformers of **4** suggest that the hydrogen bond 6'-OH---O=C-OMe places the 6'-OH in an orientation to interact with the lone pair of the pyramidalized nitrogen in the transition state. By comparison, the absence of this hydrogen bond in **3** prevents stabilization of the transition state. Moreover, the H-bond 6'-OH---HO-6 observed in the *trans* isomer of **3** places the 6'-OH in a geometry

(45) Backbone torsion angles: ω' = C-C'-N-C^α, φ = C'-N-C^α-C', ψ = N-C^α-C'-O, ω = C^α-C'-O-C. Endocyclic torsion angles: χ⁰ = C^δ-N-C^α-C^β, χ¹ = N-C^α-C^β-C^γ, χ² = C^α-C^β-C^γ-C^δ, χ³ = C^β-C^γ-C^δ-N, χ⁴ = C^γ-C^δ-N-C^α.

(46) Song, H. K.; Kang, Y. K. *J. Phys. Chem. B* **2005**, *109*, 16982.

(47) Taylor, C. M.; Hardre, R.; Edwards, P. J. B. *J. Org. Chem.* **2005**, *70*, 1306.

(48) Morozov, A.; Kortemme, T.; Tsemekhman, K.; Baker, D. *Proc. Natl. Acad. Sci. U.S.A.* **2004**, *101*, 6946.

(49) Koskinen, A. M. P.; Helaja, J.; Kumpulainen, E. T. T.; Koivisto, J.; Mansikkamäki, H.; Rissanen, K. *J. Org. Chem.* **2005**, *70*, 6447.

(50) (a) Eberhardt, E. S.; Panasiak, N., Jr.; Raines, R. T. *J. Am. Chem. Soc.* **1996**, *118*, 12261. (b) Renner, C.; Alefelder, S.; Bae, J. H.; Budisa, N.; Huber, R.; Moroder, L. *Angew. Chem., Int. Ed.* **2001**, *40*, 923.

(51) Fisher, S.; Dunbrack, R. L., Jr.; Karplus, M. *J. Am. Chem. Soc.* **1994**, *116*, 11931.

(52) Beausoleil, E.; Sharma, R.; Michnick, S. W.; Lubell, W. D. *J. Org. Chem.* **1998**, *63*, 6572.

that prevents H-bonding to the endocyclic nitrogen in the transition state, thereby leading to a higher activation energy in **3**.⁵¹

Comparison of the activation enthalpies (ΔH^\ddagger) for *cis*-to-*trans* isomerization and *trans*-to-*cis* isomerization of compounds **3–6** indicate that the kinetics of *cis/trans* isomerization is enthalpically driven. The lower (ΔH^\ddagger) observed for compound **4** when compared to **5** and **6** could be the result of a developing hydrogen bond between the hydroxymethyl substituent at C-5' and the lone pair of the pyramidalized nitrogen in the transition state. In contrast, the higher activation enthalpy observed for peptide mimic **3** when compared to reference compounds **5** and **6** could be the result of increased Coulomb repulsion induced by the Ψ dihedral angle around 153°. ^{52,53}

Previously, accelerated *cis/trans* isomerizations have been observed in model peptides containing δ -*tert*-butylproline⁵³ or pseudoproline (Ψ Pro).²² In these cases, a twisted amide bond caused by the steric strain of the bulky substituents adjacent to the endocyclic imide results in a destabilized ground state.^{22,53} In addition, the increased distance between C-5' and the heteroatom such as sulfur or oxygen leads to a shortened 5'-C-N bond in pseudoprolines.²² As a consequence, dimethyl groups at the C-5' position come closer to the isomerizing bond and may stabilize the transition state by the presence of the hydrophobic alkyl group.⁵⁴ Our results indicate that insertion of a polar group(s) at the δ -position of proline or in the form of sugar-proline hybrids provides an alternative route to control the kinetics of prolyl amide *cis/trans* isomerization.

Conclusions

We have studied the thermodynamic and kinetic properties of a series of polyhydroxylated Glc3'(S)-5'(CH₂OH)-HypHs-containing peptide mimics. Our study shows that the insertion of polar substituents capable of forming hydrogen bonds in the C-5' position of proline greatly impacts the kinetics and thermodynamics of prolyl amide *cis/trans* isomerization. DFT calculations and chemical shift temperature coefficient measurements indicate that these changes are not due to conformational changes in the pucker of the pyrrolidine ring, but rather are the result of intramolecular hydrogen bonding in water. Computational modeling of the pyrrolidine ring indicates that the pyrrolidine ring prefers a C ^{β} -exo pucker. However, close inspection of the C ^{β} -exo pucker suggests that it is closely related to the C ^{γ} -endo pucker that occurs frequently in proline-containing peptides and proteins. The preferable adoption of the prolyl amide *cis* conformation in glucose-3'(S)-hydroxy-5'(R)-hydroxymethyl proline **4** allows its use as selective *cis*-XAA-GlcProH bond inducer to chemically introduce constraint into peptides and proteins and to test the *cis*-imide bond as a structural requirement for the bioactive conformation. Moreover, the presence of the unprotected glucose moiety in GlcProH provides opportunities to explore the effect of glycosylation in unusual glycopeptides while decoration of the gluco-based polyol scaffold provides rich opportunities to tailor the physical, chemical, hydrophobic, lipophilic, nucleophilic, and pharmacodynamic properties of proline mimetics and proline-containing peptidomimetics.

(53) Halab, L.; Lubell, W. D. *J. Org. Chem.* **1999**, *64*, 3312.

(54) Albers, M. W.; Walsh, C. T.; Schreiber, S. L. *J. Org. Chem.* **1990**, *55*, 4984.

Experimental Section

(1S)-2,3,4,6-Tetrahydroxy-1'-N-acetyl-5'(S)-hydroxymethyl-enespiro[1,5-anhydro-D-glucitol-1,3'-L-proline methyl ester] (3). Compound **1** (30 mg, 0.10 mmol) was dissolved in a mixture of pyridine and acetic anhydride (1 mL, 1:1) and stirred for 12 h at room temperature. After that, the pyridine and acetic anhydride were removed in vacuo. The crude product was dissolved in methanol (1 mL) followed by addition of sodium methoxide (22 mg, 0.39 mmol) and stirred for 3 h. The solution was stirred with Amberlite IRC-50S ion-exchange resin (H⁺) for 15 min. The mixture was filtered, and filtrate was concentrated and purified by the flash column chromatography (ethyl acetate/methanol 4/1) to obtain compound **3** as a colorless oil (30 mg, 90%): [α]_D = 31.4 (*c* 1.00, MeOH); ¹H NMR (500 MHz, D₂O) δ = 1.81 (s, *cis*, 0.53H), 2.09 (s, *trans*, 2.47H), 2.11–2.34 (m, both rotamers, 2H), 3.27–3.35 (m, 2H), 3.39–3.46 (m, both rotamers, 1H), 3.50–3.66 (m, 6H), 3.67–3.72 (dd, 1H, *J* = 12.6 Hz, *J* = 2.5 Hz), 3.74–3.79 (dd, *trans*, 0.83H, *J* = 11.1 Hz, *J* = 5.3 Hz), 3.82–3.86 (dd, *cis*, 0.17H, *J* = 11.1 Hz, *J* = 5.3 Hz), 4.17–4.24 (m, both rotamers, 1H), 4.26 (s, *trans*, 0.81 H), 4.43 (s, *cis*, 0.19H); ¹³C NMR (75 MHz, D₂O) *trans*-rotamer, δ = 25.1, 25.7, 53.4, 60.2, 61.0, 63.2, 69.6, 69.9, 70.5, 74.1, 75.0, 86.0, 171.4, 174.8; *cis*-rotamer, 22.0, 24.6, 53.9, 59.7, 62.2, 63.2, 69.6, 69.9, 71.3, 74.1, 75.0, 87.5, 171.9, 174.6; HRMS calcd for C₁₄H₂₄NO₉ [M + H]⁺ 350.1451, found 350.1462.

(1S)-2,3,4,6-Tetrahydroxy-1'-N-acetyl-5'(R)-hydroxymethyl-enespiro[1,5-anhydro-D-glucitol-1,3'-L-proline methyl ester] (4). Compound **2** (35 mg, 0.11 mmol) was dissolved in a mixture of pyridine and acetic anhydride (1 mL, 1:1) and stirred for 12 h at room temperature. After that, the pyridine and acetic anhydride were removed in vacuo. The crude product was dissolved in methanol (1 mL) followed by addition of sodium methoxide (25 mg, 0.46 mmol) and stirred for 3 h. The solution was stirred with Amberlite IRC-50S ion-exchange resin (H⁺) for 15 min. The mixture was filtered, and the filtrate was concentrated and purified by the flash column chromatography (ethyl acetate/methanol 4/1) to obtain compound **4** as a colorless oil (37 mg, 92%): [α]_D = 63.9 (*c* 1.00, MeOH); ¹H NMR (500 MHz, D₂O) δ = 1.86 (s, *cis*, 1.56H), 1.94 (dd, *cis*, 0.52H, *J* = 14.3 Hz, *J* = 10.3 Hz), 1.99–2.08 (m, 1.92H), 2.37 (dd, *cis*, 0.52H, *J* = 14.3 Hz, *J* = 7.2 Hz), 2.48 (dd, *trans*, 0.48H, *J* = 14.3 Hz, *J* = 7.2 Hz), 3.25–3.35 (m, 2H), 3.38–3.45 (m, 1H), 3.53–3.75 (m, 7H), 3.80–3.88 (m, 1H), 4.04 (m, *cis*, 0.52H), 4.14 (m, *trans*, 0.48H), 4.37 (s, *cis*, 0.52H), 4.40 (s, *trans*, 0.48H); ¹³C NMR (75 MHz, D₂O) *trans*-rotamer, 21.3, 29.1, 53.6, 58.8, 61.1, 63.9, 69.7, 69.9, 70.2, 74.1, 75.3, 85.0, 172.0, 174.9; *cis*-rotamer, 21.6, 27.0, 53.7, 59.0, 61.1, 62.9, 69.8, 70.0, 71.2, 74.2, 75.4, 86.1, 172.0, 174.9; HRMS calcd for C₁₄H₂₄NO₉ [M + H]⁺ 350.1451, found 350.1456.

N-Acetyl-3(S)-hydroxy-L-proline Methyl Ester (5). To a solution of Boc-3(S)-OH-Pro-OH (100 mg, 0.43 mmol) and methyl iodide (0.08 mL, 1.29 mmol) in *N,N*-dimethylformamide was added cesium carbonate (154 mg, 0.47 mmol) and the mixture stirred for 1 h at 0 °C. The reaction was quenched with water (3 mL) and extracted with ethyl acetate (3 \times 10 mL). The combined organic layers were concentrated to afford the methyl ester, which was treated with a mixture of trifluoroacetic acid and dichloromethane (v/v, 1 mL/1 mL) and stirred for 2 h at room temperature. The mixture was concentrated in vacuo to afford the intermediate NH₂·TFA-3(S)-OH-Pro-OMe. This salt was dissolved in methanol (2 mL) and treated with triethylamine (0.12 mL, 0.86 mmol) and acetic anhydride (0.12 mL, 1.29 mmol) for 12 h at room temperature. The mixture was concentrated and purified by flash chromatography (ethyl acetate/methanol 20/1) to obtain compound **5** (78 mg, yield 96%): ¹H NMR (500 MHz, D₂O): δ = 1.82–2.10 (both isomers, m, 5H, *N*-amide methyl group and γ -protons), 3.50 (*cis*, dd, 0.43H, δ -protons, *J* = 5.78 Hz, *J* = 9.40 Hz), 3.60–3.66 (*trans*, m, 3.95H, methyl group of ester and δ -protons), 3.68 (*cis*, methyl group of ester, 0.63H), 4.24 (s, *trans*, 0.79H, α -proton),

4.41 (m, *trans*, 0.78H, β -proton), 4.47 (s, *cis*, 0.21H, α -proton), 4.55 (m, *cis*, 0.22H, β -proton); ^{13}C NMR (75 MHz, D_2O) *trans*-rotamer, $\delta = 21.4, 32.4, 46.5, 53.6, 67.4, 73.4, 172.6, 174.0$; *cis*-rotamer, $\delta = 21.7, 30.7, 44.9, 53.9, 69.2, 74.8, 172.0, 174.2$; MS (ES, $[\text{M} + \text{Na}]^+$) m/z calcd for $\text{C}_8\text{H}_{13}\text{NNaO}_4$ 210.07, found 210.13.

(*N*-acetyl-L-proline Methyl Ester (6). This compound is commercially available and used without further purification: ^1H NMR (500 MHz, D_2O) $\delta = 1.65\text{--}2.27$ (both isomers, m, 7H, *N*-amide methyl group, β and γ -protons), 3.37 (*cis*, m, 0.26H, δ -protons), 3.52 (*trans*, m, 1.74H, δ -protons), 3.58–3.70 (both isomers, partially overlapping, methyl group of ester, 3H), 4.31 (m, *trans*, 0.87H, α -proton), 4.57 (m, *cis*, 0.13H, α -proton); ^{13}C NMR (75 MHz, D_2O) *trans*-rotamer, $\delta = 21.6, 24.6, 29.6, 48.8, 53.3, 59.4, 173.3, 175.4$; *cis*-rotamer, $\delta = 22.8, 24.6, 31.0, 47.0, 53.6, 61.1, 173.7, 175.0$; MS (ES, $[\text{M} + \text{Na}]^+$) m/z calcd for $\text{C}_8\text{H}_{13}\text{NNaO}_3$ 194.08, found 194.18.

(1*S*)-2,3,4,6-Tetrahydroxy-1'-*N*-acetyl-5'(S)-hydroxymethyl-*enespiro*[1,5-anhydro-D-glucitol-1,3'-L-proline methylamide] (7). The synthetic procedure is described in the Supporting Information: $[\alpha]_{\text{D}} = 46$ (c 0.8, MeOH); ^1H NMR (500 MHz, D_2O) $\delta = 1.79$ (s, *cis*, 1.15H), 2.06 (s, *trans*, 1.85H), 2.11–2.30 (m, both rotamers, 2H), 2.56 (s, *trans*, 1.83H), 2.61 (s, *cis*, 1.17H), 3.25–3.50 (m, 4.4H), 3.54–3.70 (m, 2.6H), 3.74 (dd, *trans*, 0.64H, $J = 5.1$ Hz, $J = 11.2$ Hz), 3.74 (dd, *cis*, 0.36H, $J = 4.7$ Hz, $J = 10.7$ Hz), 4.12–4.25 (m, 2H); ^{13}C NMR (75 MHz, CD_3OD) *cis* rotamer, $\delta = 22.6, 26.7, 26.8, 61.6, 62.9, 64.7, 71.4$ (2 carbons), 74.3, 75.6, 77.3, 88.5, 171.7, 173.6; *trans* rotamer, $\delta = 22.3, 25.7, 26.7, 61.5, 62.7, 63.9, 71.4$ (2 carbons), 73.4, 75.5, 77.2, 87.2, 171.5, 173.2; HRMS calcd for $\text{C}_{14}\text{H}_{25}\text{N}_2\text{O}_8$ $[\text{M} + \text{H}]^+$ 349.1611, found 349.1626.

(1*S*)-2,3,4,6-Tetrahydroxy-1'-*N*-acetyl-5'(R)-hydroxymethyl-*enespiro*[1,5-anhydro-D-glucitol-1,3'-L-proline methylamide] (8). The synthetic procedure is described in the Supporting Information: $[\alpha]_{\text{D}} = 62.3$ (c 0.6, MeOH); ^1H NMR (500 MHz, D_2O) $\delta = 1.86$ (s, *cis*, 2.22H), 2.05 (s, *trans*, 0.78H), 2.11 (m, *cis*, 0.74H), 2.25 (m, 1.26H), 2.56 (s, *trans*, 0.78H), 2.61 (s, *cis*, 2.22H), 3.25–3.35 (m, 2H), 3.37–3.43 (m, 1H), 3.53–3.61 (m, 2.79H), 3.64–3.70 (m, 1.21H), 3.96–4.04 (m, 1H), 4.07 (s, *cis*, 0.74H), 4.09–4.18 (m, 1H), 4.19 (s, *trans*, 0.26H); ^{13}C NMR (75 MHz, CD_3OD) *cis* rotamer, $\delta = 23.1, 26.0, 26.4, 59.6, 60.7, 62.7, 71.1, 71.3, 74.5, 75.6, 77.4, 87.0, 172.9, 173.8$; *trans* rotamer, $\delta = 21.9, 28.4, 26.3, 59.3, 62.3, 63.1, 71.1, 71.6, 73.3, 75.9, 77.4, 85.5, 173.2, 173.8$; HRMS calcd for $\text{C}_{14}\text{H}_{25}\text{N}_2\text{O}_8$ $[\text{M} + \text{H}]^+$ 349.1611, found 349.1618.

Thermodynamics. The equilibrium constants for the interconversion of the *cis* and *trans* isomers of **3–6** were determined by measuring the peak area of the ^1H resonance for the two isomers.

Peak areas were measured with the program Spinworks 2.5. Experiments were conducted at 298–360 K. Equilibrium constants ($K_{\text{tr}} = \text{trans}/\text{cis}$ ratios) were calculated directly from the peak areas.

Inversion-magnetization transfer NMR experiments were performed on 500 MHz NMR spectrometer equipped with selective excitation units and ^1H and broadband heteronuclear probes. Samples of **3–6** were prepared at a concentration of 0.01 M in D_2O . The rate of prolyl peptide bond isomerization cannot be detected by this method at room temperature. Experiments were therefore conducted at elevated temperature at 356 K. Temperature settings of the spectrometer were calibrated to within 1 °C by reference to a glycol standard.

FT-IR Spectroscopy. Samples of **3–6** were prepared at concentration of 0.10 M in D_2O . Spectra were recorded on a FTIR spectrometer. Experiments were performed at 25 °C using CaF_2 in a Spectra Tech circle cell. The frequency of amide I vibrational modes was determined to within 2 cm^{-1} .

Temperature coefficient ($\Delta\delta/\Delta T$) experiment: 1D ^1H NMR spectroscopy of 17 mM solutions of **19** and **20** in 100.0% $\text{Me}_2\text{SO}-d_6$ were recorded on 500 MHz NMR spectrometer at 20 °C, and from 20 to 45 °C with increments of 5 °C, using routine techniques. Chemical shifts (δ) are expressed in ppm and calibrated with respect to the residual DMSO signal (^1H : 2.49 ppm).

Acknowledgment. This work was supported by the Natural Sciences and Engineering Research Council of Canada (NSERC) and the Canada Foundation for Innovation (CFI). We are grateful to Dr. Kirk Marat for his help with kinetic studies. We also thank Dr. Joe O'Neil for providing the Mathematica 5.0 script for analyzing the inversion-magnetization recovery experiments and Dr. Anthony Shaw for help with the FT-IR measurements.

Supporting Information Available: ^1H and ^{13}C NMR spectra of **3–8**; 1D NOE experiments of compounds **3**, **4**, **7**, and **8**. HSQC NMR spectra of **3–6**. Plots of intensity versus mixing time for the magnetization transfer experiments on **3–6**. Table of kinetic and thermodynamic data. The FT-IR spectrum of the amide-I stretch region of **3–6**. The temperature coefficient experiments for **3** and **4**. Full computational details and characterization of *cis/trans* isomers. This material is available free of charge via the Internet at <http://pubs.acs.org>.

JO9003458